Conceptual design of a 10^{13}-W pulsed-power accelerator for megajoule-class dynamic-material-physics experiments

W. A. Stygar,[1] D. B. Reisman,[1] B. S. Stoltzfus,[1] K. N. Austin,[1] T. Ao,[1] J. F. Benage,[1] E. W. Breden,[1] R. A. Cooper,[2] M. E. Cuneo,[1] J.-P. Davis,[1] J. B. Ennis,[3] P. D. Gard,[1] G. W. Greiser,[4] F. R. Gruner,[5] T. A. Haill,[1] B. T. Hutsel,[1] P. A. Jones,[1] K. R. LeChien,[6] J. J. Leckbee,[1] S. A. Lewis,[1] D. J. Lucero,[1] G. R. McKee,[1] J. K. Moore,[1] T. D. Mulville,[1] D. J. Muron,[1] S. Root,[1] M. E. Savage,[1] M. E. Sceiford,[1] R. B. Spielman,[7] E. M. Waisman,[1] and M. L. Wisher[1]

[1]*Sandia National Laboratories, Albuquerque, New Mexico 87185, USA*
[2]*General Atomics, San Diego, California 92186, USA*
[3]*NWL Capacitor Division, Snow Hill, North Carolina 28580, USA*
[4]*CSI Technologies, Vista, California 92081, USA*
[5]*Kinetech Corporation, Cedar Crest, New Mexico 87008, USA*
[6]*National Nuclear Security Administration, Washington, D.C. 20585, USA*
[7]*Idaho State University, Pocatello, Idaho 83209, USA*

(Received 25 January 2016; published 7 July 2016)

We have developed a conceptual design of a next-generation pulsed-power accelerator that is optimized for megajoule-class dynamic-material-physics experiments. Sufficient electrical energy is delivered by the accelerator to a physics load to achieve—within centimeter-scale samples—material pressures as high as 1 TPa. The accelerator design is based on an architecture that is founded on three concepts: single-stage electrical-pulse compression, impedance matching, and transit-time-isolated drive circuits. The prime power source of the accelerator consists of 600 independent impedance-matched Marx generators. Each Marx comprises eight 5.8-GW bricks connected electrically in series, and generates a 100-ns 46-GW electrical-power pulse. A 450-ns-long water-insulated coaxial-transmission-line impedance transformer transports the power generated by each Marx to a system of twelve 2.5-m-radius water-insulated conical transmission lines. The conical lines are connected electrically in parallel at a 66-cm radius by a water-insulated 45-post sextuple-post-hole convolute. The convolute sums the electrical currents at the outputs of the conical lines, and delivers the combined current to a single solid-dielectric-insulated radial transmission line. The radial line in turn transmits the combined current to the load. Since much of the accelerator is water insulated, we refer to it as Neptune. Neptune is 40 m in diameter, stores 4.8 MJ of electrical energy in its Marx capacitors, and generates 28 TW of peak electrical power. Since the Marxes are transit-time isolated from each other for 900 ns, they can be triggered at different times to construct–over an interval as long as 1 μs–the specific load-current time history required for a given experiment. Neptune delivers 1 MJ and 20 MA in a 380-ns current pulse to an 18-mΩ load; hence Neptune is a megajoule-class 20-MA arbitrary waveform generator. Neptune will allow the international scientific community to conduct dynamic equation-of-state, phase-transition, mechanical-property, and other material-physics experiments with a wide variety of drive-pressure time histories.

DOI: 10.1103/PhysRevAccelBeams.19.070401

I. INTRODUCTION

In the late 1990s, Reisman and colleagues [1] and Hall and coworkers [2,3] developed a novel experimental platform for dynamic-material-physics experiments: an inductive short-circuit load that was driven by the Z pulsed-power accelerator [4–16].

The Z machine was located at Sandia National Laboratories in Albuquerque, New Mexico, USA. Z was powered by 36 modules, each of which was driven by a Marx generator. Each module included a 5-MV laser-triggered gas switch. Each switch compressed the electrical-power pulse generated by its associated Marx, and served as the last command-triggered switch of a module. For most of the experiments that were initially conducted on Z, the 36 gas switches were triggered simultaneously to achieve a 100-ns current pulse at the load. Reisman, Hall, and colleagues instead triggered the switches at different times, to generate a several-hundred-nanosecond load-current time history with the shape required to conduct a material-physics experiment. The current pulse created a magnetic pressure between the current-carrying conductors of the load; the pressure was

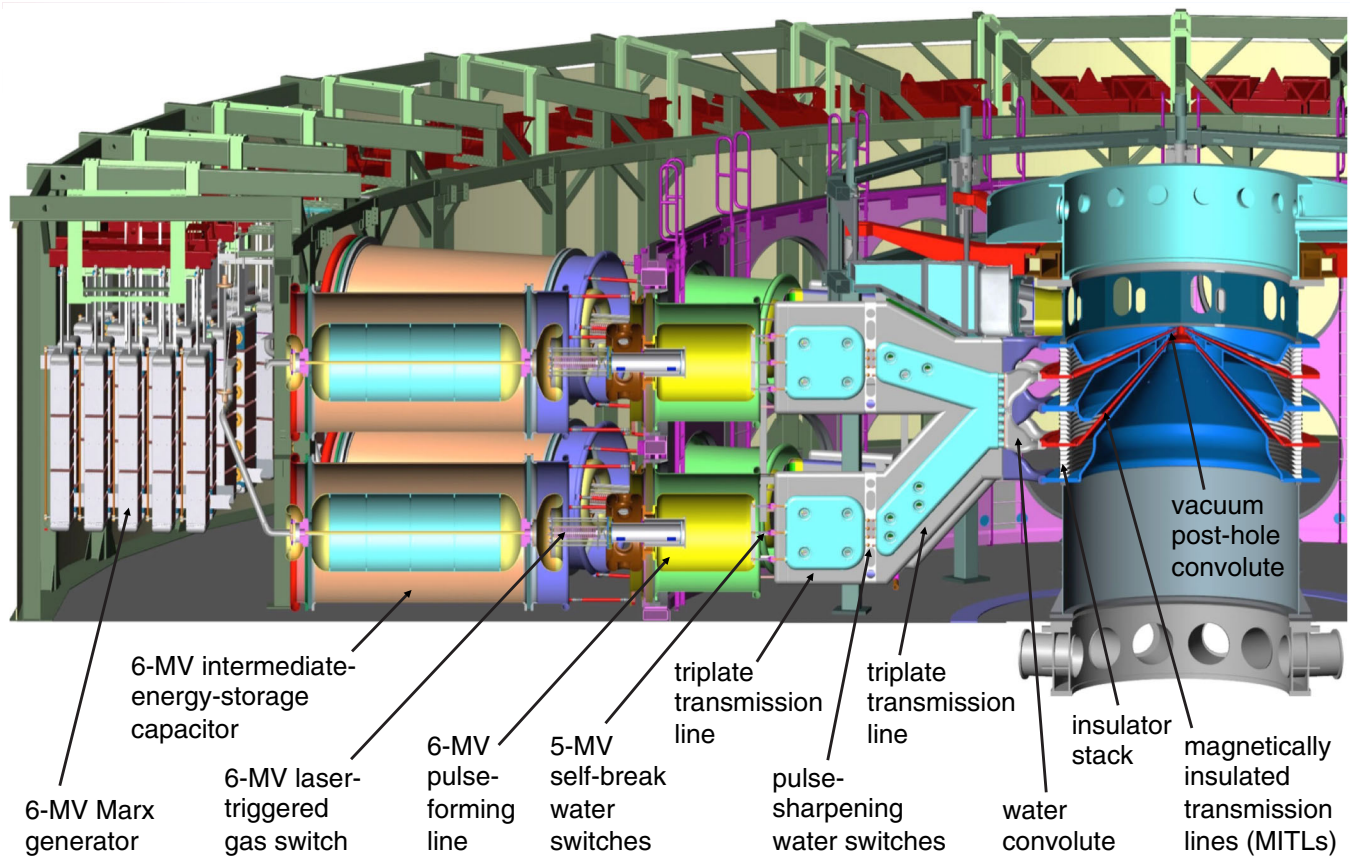

FIG. 1. Cross-sectional view of two modules of the ZR pulsed-power accelerator.

transmitted to material samples that were mechanically coupled to the load [1–3]. The new experimental platform revolutionized the field of dynamic material physics.

Afterward, a large number of material experiments were conducted on Z. Such experiments are presently being continued on Z's successor, the refurbished Z machine, which is also referred to as ZR [17–29].

Like Z, ZR is powered by 36 pulsed-power modules, each of which is driven by a Marx generator. A cross-sectional view of two ZR modules is presented by Fig. 1. As indicated by the figure, each module includes a 6-MV laser-triggered gas switch [21,28], a set of three self-break 5-MV main water switches, and a set of four self-break pulse-sharpening water switches. ZR stores 20 MJ of electrical energy in its Marx capacitors at a charge voltage of 85 kV, and achieves a peak electrical power as high as 85 TW at the accelerator's insulator stack. The stack serves as the machine's water-vacuum interface. ZR uses its 36 laser-triggered gas switches and 72 sets of water switches to shape the load-current pulse as required for a material-physics experiment. The length of the pulse is typically several hundred nanoseconds; the peak current is as high as 17 MA. Such experiments have achieved material pressures as high as 1 TPa.

The success of these experiments has motivated the development of a number of megampere-class pulsed-power accelerators that are optimized for material-science research [30–36]. These machines deliver as much as 5 MA to a load and achieve pressures as high as 100 GPa. To maximize the peak load current, the drive circuits of the machines are connected as closely as possible to the load, which minimizes the inductance of the connections. Because the drive circuits of such a configuration are strongly coupled, it is challenging for such machines to achieve the precisely shaped load-current time history required for a typical experiment.

To facilitate the creation of a wide variety of precise load-current time histories, a next-generation material-physics accelerator has been conceived and is being developed [37–41]. This machine, which we refer to as Thor, will be driven by as many as 288 independent transit-time-isolated bricks. (A brick is an *RLC* circuit that comprises a switch and two capacitors connected electrically in series.) Thor will store as much as 230 kJ in its capacitors, generate a peak electrical power as high as 1.4 TW, and deliver as much as 7 MA to a physics load.

Since the bricks are transit-time isolated from each other, they can be triggered at different times to construct, with a high-degree of precision, the specific load-current time history required for a given experiment. (When the load has a constant impedance, and nonlinear effects within the rest of the Thor circuit can be neglected, the time history of the load current is simply a linear combination of the

time-shifted current pulses generated by the bricks.) Hence Thor is a megampere-class arbitrary waveform generator, one that will achieve material pressures on the order of 170 GPa.

The scientific community is interested in increasing the pressures at which such experiments can be conducted by an order of magnitude, to 1 TPa. Such pressures require peak currents of approximately 20 MA, which can be achieved by ZR. However, ZR is used to drive a wide variety of high-energy-density-physics experiments in support of the U.S. National Nuclear Security Administration's Stockpile Stewardship Program. Hence only a limited number of material-physics experiments can be conducted on ZR each year.

It might appear that the most direct approach to increasing substantially the rate at which terapascal-class experiments can be conducted would simply be to build another ZR accelerator. For the following reasons, we propose in this article an alternate approach.

ZR represents the state of the art of *conventional* pulsed-power-accelerator technology. The LC time constant $[(LC)^{1/2}]$ of each ZR Marx is 750 ns. (The quantities L and C are the series inductance and capacitance of each Marx, respectively.) Hence each ZR Marx generates an electrical power pulse with a temporal width on the order of 1 μs. Since material-physics experiments require each of ZR's 36 modules to generate a power pulse with a width on the order of 100 ns, each module uses its laser-triggered gas switch, self-break water switches, and associated hardware to compress the pulse. The compression hardware, illustrated by Fig. 1, reduces by an order of magnitude the width of the pulse generated by each Marx.

Although the hardware successfully compresses the pulse, it introduces impedance mismatches, which cause multiple reflections of the pulse within the accelerator. The mismatches and reflections complicate the machine design (as suggested by Fig. 1), reduce the energy and power efficiencies of the accelerator, reduce accelerator-component lifetimes, and increase the effort required to maintain and operate the machine.

The increased complexity inherent in the pulse-compression hardware also increases the difficulty of conducting predictive circuit and electromagnetic simulations of an accelerator shot, and thereby achieving the precise load-current time history required for a given experiment.

The difficulty is increased by the fact that the gas and water switches of each ZR module are not transit-time isolated from the switches in the other modules. Hence a fraction of the electrical power generated by the modules that are triggered first for an accelerator shot reflects from the ZR center section (i.e., the centrally located inductive vacuum section of ZR), propagates upstream in the modules triggered later in the pulse, interacts with the switches in these modules, and affects the performance of the switches. The difficulty of conducting predictive simulations is increased as well by current loss within ZR's system of magnetically insulated transmission lines (MITLs). The loss is a significant fraction of the total current, and suffers from substantial stochastic shot-to-shot fluctuations.

In addition, ZR was optimized to drive inertial-confinement-fusion experiments. Since such experiments generate voltages as high as 5 MV near the physics load, the ZR center section comprises a 3.5-m-diameter MITL system and a 2-m-height vacuum insulator stack. The initial inductance of the center section is 20 nH. Such a large and inductive center section is not required for material-physics experiments, which generate substantially lower voltages. Hence the ZR center section unnecessarily reduces the energy efficiency of such experiments, since current delivered to the load must also fill the 20-nH center-section inductance with magnetic field.

Furthermore, when a ZR material-physics experiment is conducted with a hazardous material within the load, the ZR MITLs require use of an active explosively closed containment system. The MITL system includes a short single MITL that delivers the ZR-accelerator current to the load. To deliver this current, the anode-cathode (AK) gap of the MITL must be open during the current pulse. The containment system uses explosives to close this gap after the experiment has been completed. Hence in the unlikely event of a containment-system failure, the hazardous substance would escape the containment system through the MITL gap and contaminate the ZR center section.

Thus instead of building another ZR machine, we propose to design and build an accelerator that is *optimized* for driving megajoule-class 1-TPa material-physics experiments.

We propose to base the design of the new machine upon the architecture used to develop the Thor accelerator. The architecture is founded on three fundamental concepts: single-stage electrical-pulse compression, impedance matching, and transit-time-isolated drive circuits [37–43].

We propose that the LC time constant of each drive circuit that powers the new accelerator be ~100 ns, so that the electrical-power pulse generated by each circuit does not require additional compression. We also propose that, to the extent possible, the transmission lines that transport the power pulse from the drive circuits to the load be impedance matched throughout. This approach minimizes reflections within the accelerator, and maximizes the efficiency at which electrical energy and power are delivered to the load. In addition, we propose that the machine be powered by ~600 drive circuits that are transit-time isolated over time intervals of interest. This would make it possible to construct, with unprecedented precision and reproducibility, the specific load-current time history required for a given experiment.

In this article, we describe a conceptual design of such an accelerator. Since much of the accelerator is water insulated, we refer to it as Neptune [38]. The Neptune machine

has an energy efficiency that, for dynamic-material-physics experiments, is 2.4 times greater than that of ZR. The principal goal of Neptune is to achieve material pressures on the order of 1 TPa. Accelerators founded on the Neptune concept will allow the international scientific community to conduct dynamic equation-of-state, phase-transition, mechanical-property, and other material-physics experiments with a wide variety of drive-pressure time histories. Because Neptune can deliver on the order of 1 MJ of electrical energy to the load, such experiments can be conducted on centimeter-scale samples with drive-pressure time histories that extend as long as 1 μs.

The conceptual design of Neptune is outlined by Sec. II. This is a *point* design; no attempt has yet been made to vary the electrical parameters and geometry of the accelerator configuration to develop an *optimized* design; i.e., one that maximizes the performance of the accelerator for a given cost. A circuit model of Neptune is presented by Sec. III; predictions of the model are summarized by Sec. IV.

Given the cost of an accelerator such as Neptune, it is critical that the accelerator deliver—as efficiently as possible—electrical energy initially stored by its capacitors to the physics load. Section V proposes a definition of the energy efficiency of a coupled Neptune-load system, and discusses how the efficiency might be increased. Suggestions for future work are presented by Sec. VI.

The Appendix develops an estimate of the Neptune-output impedance that maximizes the peak current delivered to the load. Numbered equations of this article are in SI units throughout.

II. CONCEPTUAL DESIGN OF NEPTUNE

The conceptual design of Neptune is illustrated by Fig. 2. Cross-sectional views of a three-dimensional model of Neptune are presented by Figs. 3 and 4. As suggested by these figures, the conceptual design comprises the following components: 600 impedance-matched Marx generators, 600 water-insulated coaxial-transmission-line impedance transformers, a system of 12 water-insulated conical transmission lines, a water-insulated sextuple-post-hole convolute, a solid-dielectric-insulated radial transmission line, and the physics load. The outer diameter of the accelerator is 40 m.

The 600 Marx generators, which are azimuthally and axially distributed, serve as Neptune's prime power source. Each Marx comprises eight bricks that are connected electrically in series, and drives an impedance-matched transmission line. (The impedance-matched-Marx concept is described in Sec. III.) Each brick consists of two 100-kV 100-nF capacitors connected in series with a single (normally open) 200-kV field-distortion gas switch [44]. Each Marx is located within a ground-potential enclosure that has a volume of 0.6 m $\times$ 0.8 m $\times$ 2.4 m.

Since each of the 600 Marxes comprises eight bricks, the accelerator is driven by 4800 bricks altogether. Each of the accelerator's 4800 switches could be triggered by a 100-kV pulse delivered by a 200-Ω transmission line. Hence the peak electrical power required to trigger all the switches is 0.24 TW, which is a small fraction of the total accelerator power.

Each Marx drives the *upstream* end of a water-insulated coaxial-transmission-line impedance transformer [42,43,45,46]. The interface between each Marx and its associated coax is located at a radius of 17.6 m.

As suggested by Figs. 2–4, the *downstream* ends of the 600 coaxes are connected to a system of 12 water-insulated conical transmission lines, which are electrically in parallel. The conical lines are arranged as a stack of six conical

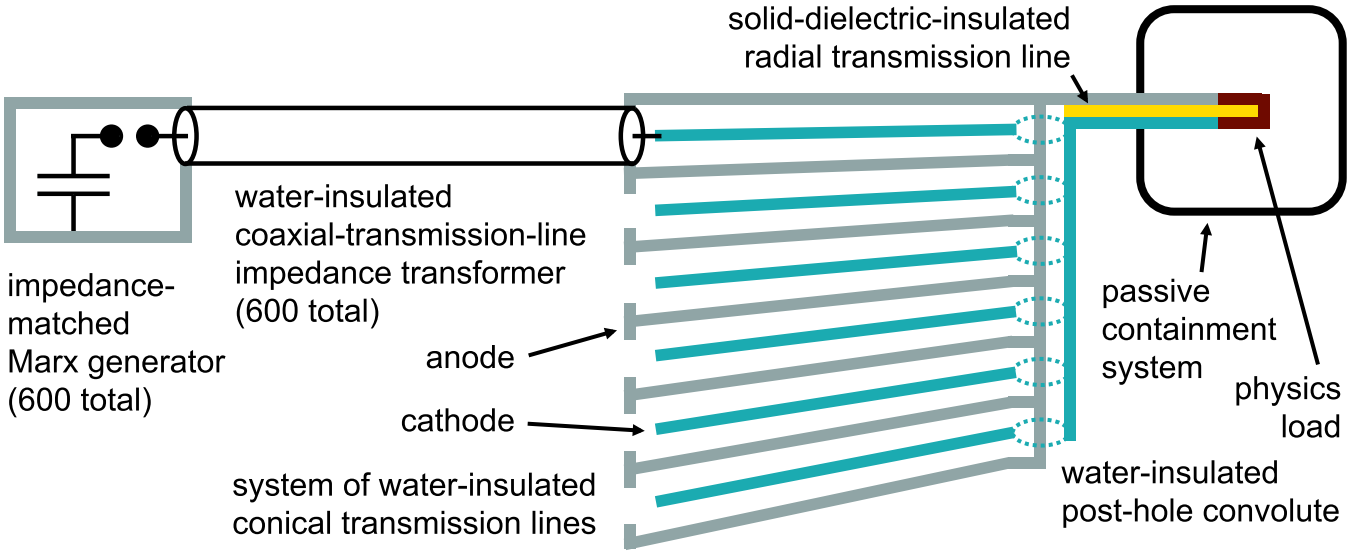

FIG. 2. Conceptual design of Neptune. Since the design includes no MITLs, it has negligible current loss and enables use (on shots conducted with a hazardous material) of a passive containment system, one that is always closed.

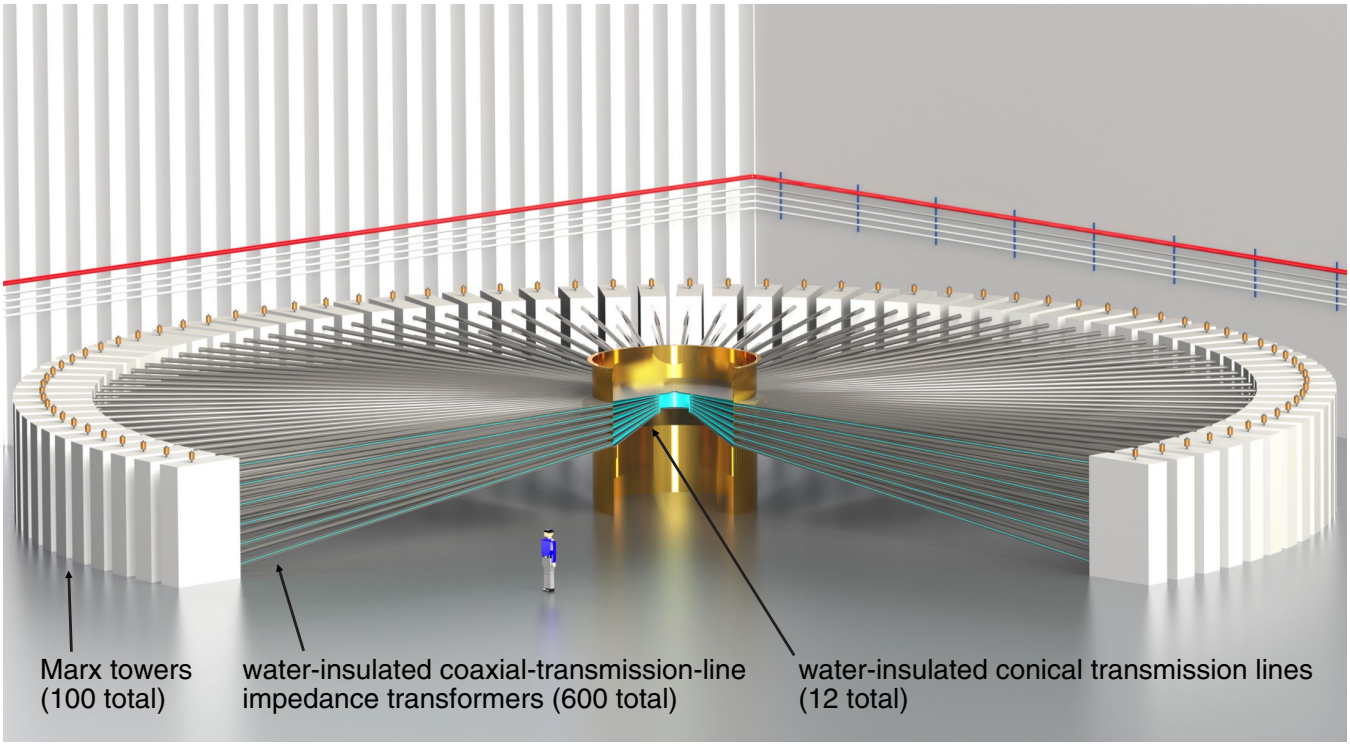

FIG. 3. Cross-sectional view of a three-dimensional model of Neptune. Each Marx tower includes six Marx generators.

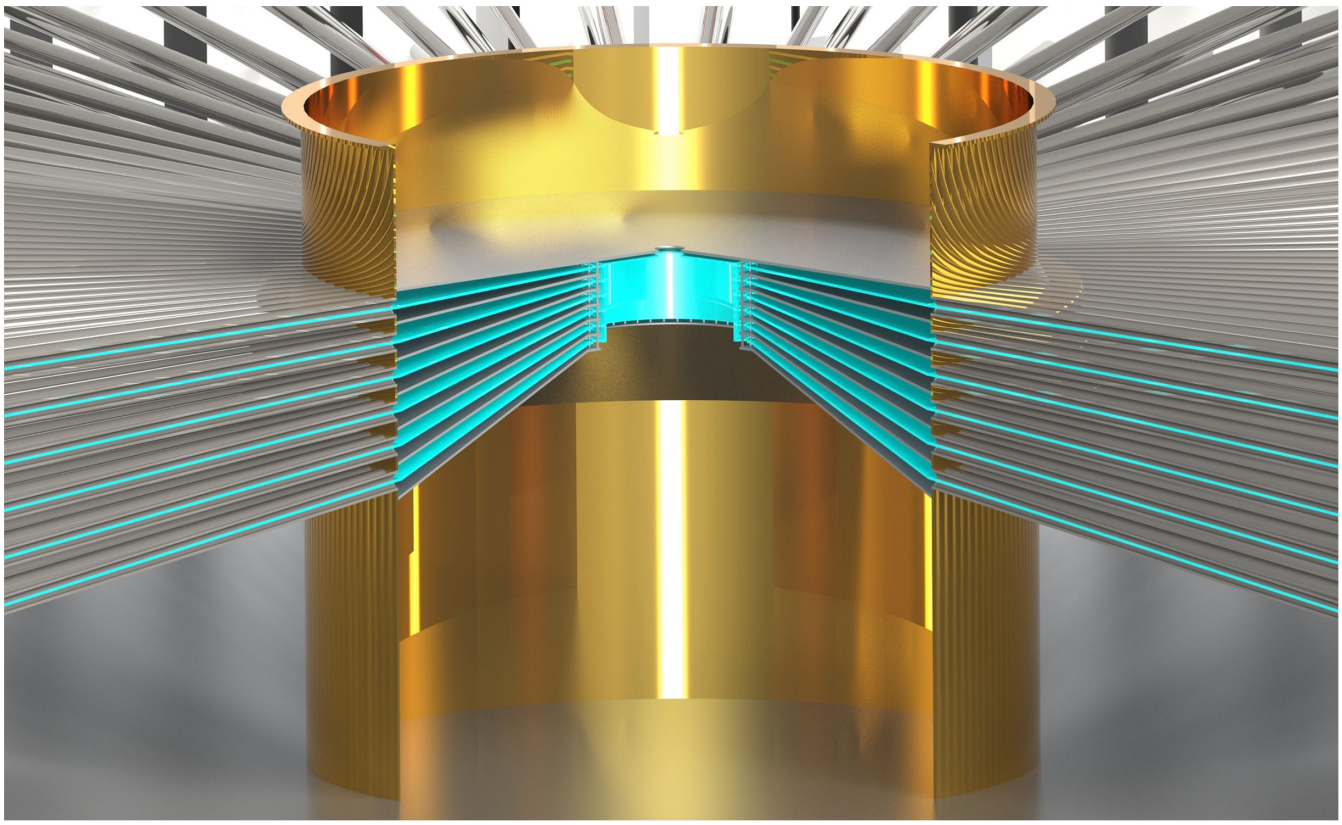

FIG. 4. Cross-sectional view of Neptune's six-level conical-transmission-line system and post-hole convolute.

pairs. The two outer conductors of each pair are anodes; the single inner conductor is a cathode. One hundred coaxes connect to each of the six conical pairs at the outer radius of the conical-line system. The outer radius of the conical system is 2.5 m; the conical lines extend radially inward to $r = 70.1$ cm. Over this radial extent, the AK gap of each conical line is proportional to the radius: at $r = 2.5$ m, the AK gap is 13.2 cm; at $r = 70.1$ cm, the AK gap is 3.69 cm. Hence over this distance the impedance of each conical line is a constant 0.353 Ω.

At $r = 70.1$ cm, the conical lines connect to a water-insulated 45-post sextuple-post-hole convolute. The convolute extends radially from $r = 70.1$ cm to $r = 61.9$ cm. The convolute posts are located on a 66-cm radius. As suggested by Figs. 2 and 4, the convolute connects the twelve conical lines in parallel, combines the currents at the outputs of the conical lines, and delivers the combined current to a single solid-dielectric-insulated radial transmission line.

The convolute connects to the radial line at a 61.9-cm radius; the radial line extends from $r = 61.9$ cm to $r = 2$ cm. The line could be insulated with a combination of dielectrics, such as Rexolite and biaxially oriented polypropylene. The line transmits the accelerator's combined current to the physics load at $r = 2$ cm. The radial-line and load concepts are founded on the seminal designs developed by Ao and colleagues [30].

The load consists of a set of conductors that form an inductive short circuit [1–3,30–41]. The current delivered to such a load creates a magnetic pressure between the load's conductors, which is used to drive the experiment. A discussion of the wide variety of load designs that could be driven by Neptune is outside the scope of the present article. To develop the conceptual design of Neptune, we made the simplifying assumption that the impedance of a typical material-physics load can be represented by an effective constant value. For such a design effort, one could use the energy-weighted impedance as defined by Waisman, Reisman, and colleagues [41].

III. CIRCUIT MODEL OF NEPTUNE

We have developed a circuit model of Neptune using the SCREAMER circuit code [47–49]. The model is illustrated by Fig. 5. Neptune is driven by 600 impedance-matched Marx generators; the circuit model of a single such Marx is illustrated by Fig. 6. The circuit elements of these models are discussed in this section.

The quantity C_M (of Figs. 5 and 6) is the capacitance of a single Neptune Marx generator, and is given by the following expression:

$$C_M = \frac{C_b}{n_b}, \tag{1}$$

where

$$C_b = 50 \text{ nF}, \tag{2}$$

$$n_b = 8. \tag{3}$$

The quantity C_b is the capacitance of a single brick (which includes two 100-nF capacitors connected in series) and n_b is the number of bricks per Marx.

We define V_M to be the initial charge voltage across a Marx:

$$V_M = n_b V_b, \tag{4}$$

$$V_b = 200 \text{ kV}, \tag{5}$$

where V_b is the initial voltage across a single brick. The initial voltage is applied to each brick in a balanced

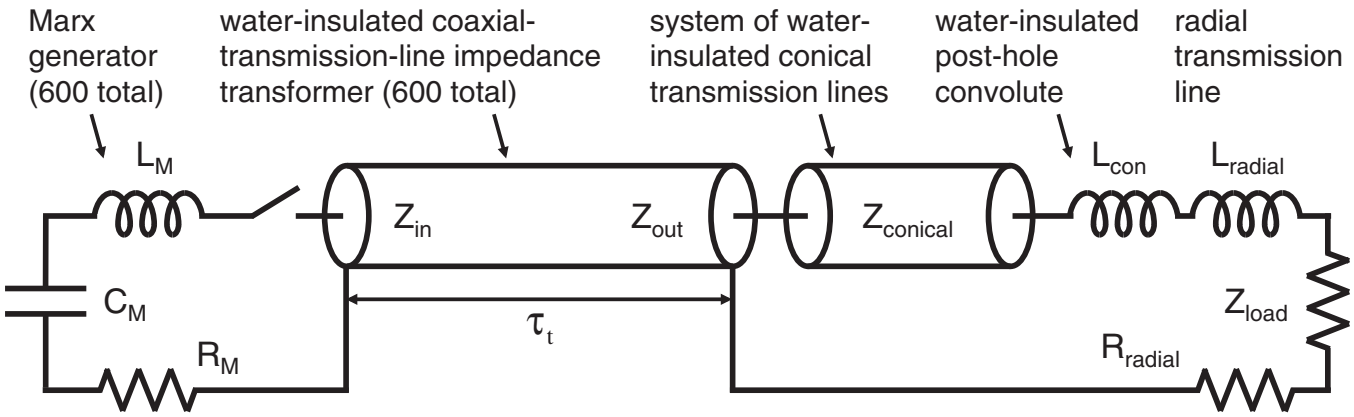

FIG. 5. Circuit model of the Neptune accelerator. The quantities L_M, C_M, and R_M are the series inductance, capacitance, and resistance, respectively, of a single Marx generator; Z_{in} and Z_{out} are the input and output impedances, respectively, of a single water-insulated coaxial-transmission-line impedance transformer; Z_{conical} is the impedance of the system of twelve parallel water-insulated conical transmission lines; L_{con} is the inductance of the water-insulated post-hole convolute; L_{radial} is the initial inductance of the solid-dielectric-insulated radial transmission line; Z_{load} is the load impedance (which in this article is assumed to be constant); and R_{radial} is a resistive circuit element that models the time-dependent energy loss to the two radial-transmission-line electrodes.

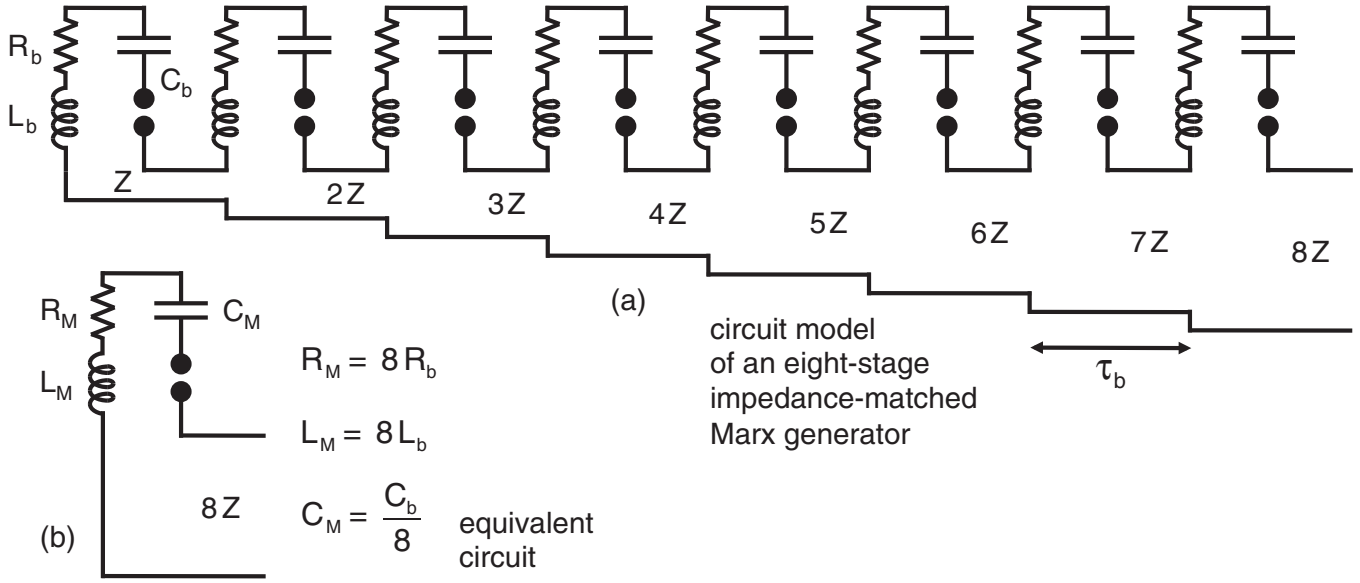

FIG. 6. (a) Circuit model of an impedance-matched Marx generator. (b) Equivalent circuit of such a Marx, when each brick of the circuit is triggered at time τ_b after the brick immediately upstream is triggered. The quantity τ_b is the one-way transit time of the transmission-line segment that connects two adjacent bricks.

manner, so that +100 kV appears across one of the brick's capacitors, −100 kV across the other, and 200 kV across the brick's switch [50]. (Hence each brick can be considered as a single two-stage Marx [50].) The total energy stored by the Neptune capacitors E_{total} is one measure of the size of the accelerator:

$$E_{\text{total}} = \frac{1}{2} n_M C_M V_M^2 = \frac{1}{2} n_t C_b V_b^2, \tag{6}$$

$$n_M = 600, \tag{7}$$

$$n_t = n_b n_M = 4800, \tag{8}$$

where n_M is the total number of Marx generators, and n_t is the total number of bricks in the machine.

We assume the series inductance and resistance of a single Marx, L_M and R_M respectively, can be approximated as constants:

$$L_M = n_b L_b, \tag{9}$$

$$L_b = 160 \text{ nH}, \tag{10}$$

$$R_M = n_b R_b, \tag{11}$$

$$R_b = 0.3\ \Omega, \tag{12}$$

where L_b and R_b are the series inductance and resistance of a single brick.

The brick inductance and resistance are functions of the spatially dependent electron, ion, and neutral-particle temperatures and densities of the current-carrying plasma channels within the brick's switch. Hence the inductance and resistance must be time dependent. However, over the 100-ns time interval of interest, the performance of a brick can be approximated with reasonable accuracy by using effective constant values for the inductance and resistance. Equations (10) and (12) give the assumed effective values.

Each Marx drives a water-insulated coaxial-transmission-line impedance transformer [42,43,45,46]. The optimum input impedance of a single coax can be calculated as follows [42,43]:

$$Z_{\text{in}} = 1.10\sqrt{\frac{L_M}{C_M}} + 0.80 R_M. \tag{13}$$

We define the optimum impedance to be that which maximizes the peak forward-going power at the input to the coax. According to Eqs. (1)–(3) and (9)–(13),

$$Z_{\text{in}} = 17.7\ \Omega. \tag{14}$$

The total length of each coaxial impedance transformer is 15.1 m. At frequencies of interest the dielectric constant of water is 80; therefore, the one-way transit time of the transformers is 450 ns:

$$\tau_t = 450 \text{ ns}. \tag{15}$$

For the conceptual design discussed in this article, we assume the water resistivity is so large that resistive losses due to the water insulation of the accelerator's coaxial lines, conical lines, and convolute can be neglected.

We use Eq. (A5) to obtain an *initial* estimate of the value of Z_{out} that maximizes the peak electrical power delivered by the accelerator to the load. Using this estimate as

an initial value, we determined through iterative circuit simulations that for the circuit described above, the performance of Neptune is nearly optimized when

$$Z_{\text{out}} = Z_{\text{in}}. \tag{16}$$

In general, the value of Z_{out} that optimizes the electrical performance of the coupled accelerator-load system is not equal to Z_{in}, which is the impedance of a Marx. It is often the case that the most-convenient impedance for a prime power source is not the optimum impedance to drive a load. However, for the Neptune concept outlined herein, we were able to design the prime power source to have an impedance that delivers near-optimum system performance when $Z_{\text{out}} = Z_{\text{in}}$. Such a design simplifies fabrication of the coaxial transmission lines and reduces the cost of the accelerator. We observe that even when $Z_{\text{out}} = Z_{\text{in}}$, the coaxial lines continue to serve as impedance transformers, with a voltage-transformer ratio of 1:1.

To optimize the peak power delivered by the system of coaxial impedance transformers to the system of conical transmission lines, it is clear the impedance of the conical system must equal Z_{out}/n_M:

$$Z_{\text{conical}} = \frac{Z_{\text{out}}}{n_M}. \tag{17}$$

The quantity L_{con} of Fig. 5 is the inductance of the convolute, which we estimate using the following relation:

$$\frac{1}{2} L_{\text{con}} I_{\text{con}}^2 = \frac{1}{2\mu_0} \int_V B_{\text{con}}^2 dV. \tag{18}$$

In this expression I_{con} is the total current flowing within the convolute, μ_0 is the permeability of free space, B_{con} is the spatially dependent magnetic field within the convolute, and V is the convolute volume. Using Eq. (18) we estimate the convolute inductance to be approximately 1.4 nH:

$$L_{\text{con}} = 1.4 \text{ nH}. \tag{19}$$

The quantity L_{radial} is the initial inductance of the solid-dielectric-insulated radial transmission line. To estimate this inductance, we assume the line extends radially from r_{out} to r_{in}, and the line's AK-gap g is a linear function of r. We also make the simplifying assumption that the current within the line is azimuthally symmetric. Under these conditions

$$g = ar + b, \tag{20}$$

$$L_{\text{radial}} = \frac{\mu_0}{2\pi} \left[a(r_{\text{out}} - r_{\text{in}}) + b \ln\left(\frac{r_{\text{out}}}{r_{\text{in}}}\right) \right], \tag{21}$$

where a and b are constants. Assuming $r_{\text{out}} = 61.9$ cm and $r_{\text{in}} = 2$ cm, and that the line's AK gaps are 0.5 and 0.1 cm at r_{out} and r_{in}, respectively, we estimate the initial inductance of the radial line to be 1.4 nH:

$$L_{\text{radial}} = 1.4 \text{ nH}. \tag{22}$$

The convolute volume V scales approximately as the radius r at which the convolute is located; the magnitude of the magnetic field within the convolute scales inversely with r. Hence Eq. (18) suggests L_{con} scales approximately as $1/r_{\text{out}}$, and that we could reduce L_{con} by increasing the radius at which the convolute is located. However, as suggested by Eq. (21), L_{radial} is an increasing function of r_{out}; consequently, moving the convolute to a larger radius increases L_{radial}. In an optimized electrical design $L_{\text{con}} \sim L_{\text{radial}}$, which minimizes the sum $L_{\text{con}} + L_{\text{radial}}$.

The resistive circuit element R_{radial} of Fig. 5 accounts for energy loss to the two radial-transmission-line electrodes, which are operated at peak lineal current densities that exceed 1 MA/cm. This resistance, which is time dependent, is calculated in a self-consistent manner by SCREAMER using Eq. (35) of Ref. [51]. This equation accounts for energy loss due to Ohmic heating of the radial electrodes, diffusion of magnetic field into the electrodes, $\mathbf{j} \times \mathbf{B}$ work on the electrodes, and the increase in the inductance of the radial line due to electrode motion [51].

The element Z_{load} of Fig. 5 is the *effective* load impedance. To develop the conceptual design outlined in this article, we assumed this element can be modeled as having a constant 18-mΩ impedance:

$$Z_{\text{load}} = 18 \text{ m}\Omega. \tag{23}$$

This would be the effective impedance associated with an experiment for which the characteristic load inductance is several nanohenries, and the characteristic time over which the load inductance and current increase substantially is several hundred nanoseconds. The 18-mΩ value is comparable to the energy-weighted impedance calculated for loads of interest by Waisman, Reisman, and coworkers [41].

It is clear that the total electrical energy Neptune is required to store, and the total energy delivered to the load, each scale approximately as the product of the peak load current squared I_{peak}^2, the effective load impedance Z_{load}, and the temporal width of the current pulse. When the current delivered to a constant-impedance load is a linear ramp, the energy delivered to the load can be estimated as follows:

$$E_{\text{load}} = \frac{1}{3} I_{\text{peak}}^2 Z_{\text{load}} \tau_{\text{load}}, \tag{24}$$

where τ_{load} is the time required for the current to increase from zero to its peak value.

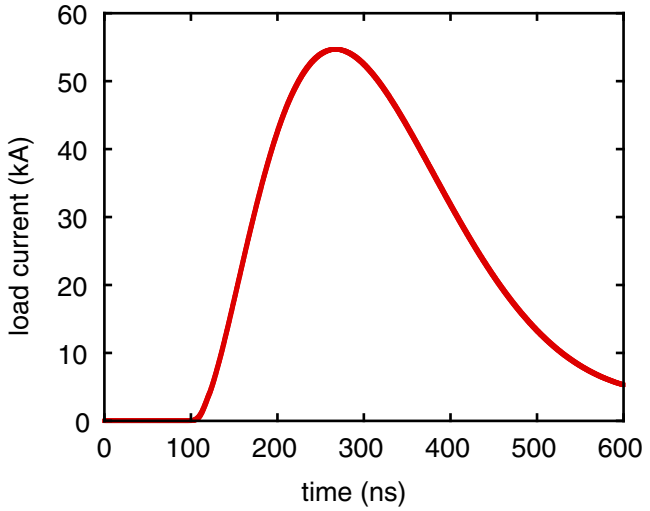

FIG. 7. Simulated load-current time history for a Neptune shot conducted with a single Marx generator. The peak current is 55 kA.

IV. RESULTS OF NEPTUNE-CIRCUIT SIMULATIONS

To obtain the current delivered to the load by a single Neptune Marx generator, we used SCREAMER to simulate a Neptune shot conducted with a single Marx. The single-Marx load-current time history is plotted by Fig. 7. This current assumes the load has a constant 18-mΩ impedance. Assuming such a load, and that nonlinear effects of R_{radial} and other elements of the Neptune circuit can be neglected, the load-current time history is a linear combination of 600 time-shifted current pulses, each of which is nominally identical to that plotted by Fig. 7.

Results of a SCREAMER simulation of a Neptune shot conducted with 600 Marx generators and a constant-impedance 18-mΩ load are summarized by Table I. For this calculation, the 600 Marxes are triggered at different times as required to achieve a peak load current of 20 MA in a pulse that rises linearly in 380 ns. The current time history is plotted by Fig. 8.

To minimize the probability of dielectric failure in Neptune's water-insulated coaxial lines, conical lines, and post-hole convolute, it is necessary for these elements to satisfy everywhere the following relation [52,53]:

$$E_w \tau_w^{0.330} \leq 1.13 \times 10^5. \tag{25}$$

At a given location within these elements the quantity E_w is the peak value in time of the average electric field, and τ_w is the full temporal width of the voltage pulse at 63% of its peak value [52,53]. {Like the other numbered equations in this article, Eq. (25) is in SI units. Different units are used in Refs. [52,53].} The SCREAMER results suggest Eq. (25) is satisfied throughout the accelerator over the time interval of interest.

TABLE I. Summary of Neptune accelerator and load parameters for a shot that delivers 20 MA to an 18-mΩ load in a 380-ns linear-ramp current pulse.

Parameter	Value
Outer accelerator diameter	40 m
Initial energy storage E_{total}	4.8 MJ
Peak voltage at the input to each of the 600 17.7-Ω coaxial-transmission-line impedance transformers	910 kV
Peak current at the input to each coax	51 kA
Peak power at the input to each coax	46 GW
Total accelerator current	31 MA
Total accelerator power	28 TW
Outer diameter of the conical-line system	5 m
Impedance of the conical system	29.4 mΩ
Peak voltage at the input to the conical system	570 kV
Peak current at the input to the conical system	18 MA
Peak power at the input to the conical system	10 TW
Post-hole-convolute inductance	1.4 nH
Radial-transmission-line inductance	1.4 nH
Effective load impedance	18 mΩ
Peak voltage at the input to the load	360 kV
Peak load current	20 MA
Load-current rise time	380 ns
Peak power at the input to the load	7.2 TW
Total energy delivered to the load at peak load current	1.0 MJ
Energy efficiency at peak load current	21%
Total energy delivered to the load at the time the current has returned to zero	1.8 MJ
Energy efficiency at the time the load current has returned to zero	38%

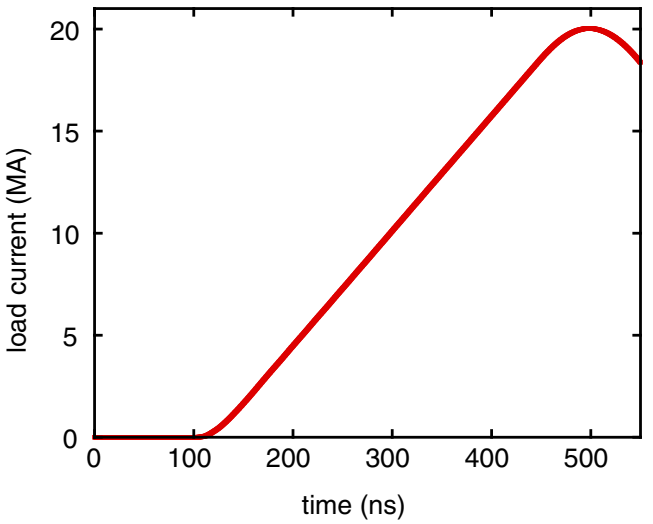

FIG. 8. Simulated load-current time history for a Neptune shot conducted with 600 Marx generators. The Marxes are triggered as required to achieve a 380-ns linear current ramp. The peak current is 20 MA.

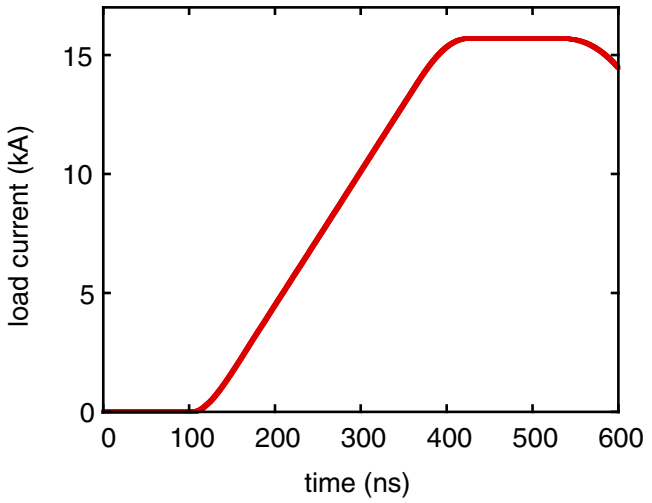

FIG. 9. Simulated load-current time history for a Neptune shot conducted with 600 Marx generators. The Marxes are triggered as required to achieve a 300-ns linear current ramp followed by a top that is flat to ±0.5% for 150 ns. The peak current is 15.7 MA.

We have not yet determined whether the water insulation within the accelerator will suffer one or more dielectric failures after the time interval of interest, or assessed the effects such breakdowns would have on accelerator-component lifetimes. We note that the ZR accelerator includes water-section energy diverters that are designed to dissipate safely electrical energy remaining in the accelerator after the time of interest; we may be required to develop such diverters for Neptune as well.

To illustrate Neptune's pulse-shaping capability, we also designed a Neptune shot that achieves a load current that rises linearly for 300 ns, and is thereafter flat to ±0.5% for 150 ns. The peak current is 15.7 MA. The load-current time history is plotted by Fig. 9.

Load-current time histories required for Neptune experiments will be achieved as described by [41].

V. ENERGY EFFICIENCY OF THE NEPTUNE-LOAD SYSTEM

The energy efficiency of the coupled Neptune-load system η_a is a function of time; we define the efficiency at time t as follows:

$$\eta_a(t) \equiv \frac{\int_0^t P_{\text{load}} dt}{E_{\text{total}}}. \tag{26}$$

The quantity P_{load} is the time-dependent electrical power delivered to the load.

Estimates of the accelerator efficiency η_a for one of the Neptune-load configurations considered in the previous section are included in Table I. An energy accounting for this configuration is presented by Table II. Given the cost of an accelerator such as Neptune, maximizing the energy efficiency of the coupled accelerator-load system will be one of the principal goals of the accelerator-design effort.

TABLE II. Energy accounting at peak load current for a Neptune shot that delivers a 380-ns linear-ramp current pulse to an 18-mΩ load. The peak current is 20 MA. The energy efficiency of the coupled accelerator-load system at peak current is 21%. The efficiency could be increased by reducing R_M, L_{con}, L_{radial}, and R_{radial}. The energy efficiency increases after peak current; however, this component of the load-current time history may not be useful for an experiment.

Circuit element	Energy
Energy dissipated by the Marx resistances R_M	0.61 MJ
Energy stored in the Marx inductances L_M	0.00 MJ
Energy stored in the Marx capacitances C_M	0.00 MJ
Energy stored in the coaxial transmission lines	2.10 MJ
Energy stored in the conical transmission lines	0.36 MJ
Energy stored in L_{con}	0.28 MJ
Energy stored in L_{radial}	0.28 MJ
Energy dissipated by R_{radial}	0.16 MJ
Energy delivered to Z_{load}	1.01 MJ
Total	4.80 MJ

It is clear that the efficiency of the conceptual design outlined herein could be increased by reducing the energy dissipated in resistances throughout the accelerator. More specifically, the efficiency could be increased by reducing R_M and R_{radial}. The efficiency could also be increased by reducing the parasitic inductances L_{con} and L_{radial}.

VI. SUGGESTIONS FOR FUTURE WORK

The conceptual design presented in this article suggests it is possible to build a 28-TW accelerator that can deliver efficiently 1 MJ and 20 MA to material-physics experiments. Such experiments are expected to achieve–in centimeter-scale samples–material pressures as high as 1 TPa.

The design is a point design; i.e., one that is self-consistent but not optimized. The design is intended to serve as a starting point for the development of an optimized final design. The optimized design should address not only electrical performance but also safety, diagnostic, mechanical, operational, and cost considerations.

We recommend that such an accelerator-design effort determine the optimum number of Marx generators, number of bricks per Marx, capacitance per brick, and number of conical-transmission-line levels.

In addition, we recommend that the design effort include the following activities: (1) development of a detailed transmission-line-circuit model of the entire accelerator, from the Marx generators to the load; (2) development of a 3D electromagnetic model of the entire accelerator; (3) development of a 3D mechanical model of the accelerator; (4) development of a 3D magnetohydrodynamic (MHD) model of the accelerator's solid-dielectric-insulated

radial transmission line; (5) development of 3D MHD models of the advanced physics loads that will be fielded on the accelerator; (6) demonstration that the circuit, electromagnetic, mechanical, and MHD models listed above are predictive, which would indicate that the coupled accelerator-load system will perform as intended; (7) continued development of advanced capacitors, switches, capacitor-charge resistors, switch-trigger resistors, switch-trigger pulse generators, coaxial-transmission-line impedance transformers, conical transmission lines, post-hole convolutes, radial transmission lines, physics loads, and post-pulse energy diverters for the accelerator; (8) design, fabrication, assembly, and commissioning of a single full-scale accelerator module (the module would include a full-scale Marx generator and full-length coaxial impedance transformer); (9) demonstration that the module meets all safety, electrical, mechanical, diagnostic, reliability, operational, and cost requirements; (10) development of a passive containment system for experiments conducted with hazardous materials (the system would not require explosives, and be closed for the entire duration of the accelerator shot).

ACKNOWLEDGMENTS

The authors gratefully acknowledge the following for invaluable contributions: Farhat Beg, Mike Campbell, Christine Coverdale, David Fehl, Dawn Flicker, Doug Fulton, Ron Gilgenbach, Mark Gilmore, Clint Hall, David Hammer, Mark Herrmann, Robert Hohlfelder, Dan Jobe, Michael Jones, Kirk Kielholtz, Joel Lash, Jane Lehr, Ray Leeper, Finis Long, John Maenchen, Keith Matzen, Mike Mazarakis, Bob McCrory, John Porter, David Sandoval, Ray Scarpetti, Edl Schamiloglu, Ralph Schneider, Jens Schwarz, Dan Sinars, Pete Wakeland, and Joe Woodworth. We are also extremely indebted to our many other colleagues at the following organizations for their gracious and sustained scientific support: Sandia National Laboratories, ASR Corporation, Barth Electronics, C-Lec Plastics, Cornell University, CSI Technologies, EG&G, General Atomics, Idaho State University, Kinetech Corporation, L-3 Communications, Laboratory for Laser Energetics at the University of Rochester, Lawrence Livermore National Laboratory, Los Alamos National Laboratory, National Nuclear Security Administration, National Security Technologies, Naval Research Laboratory, NWL Capacitor Division, Raytheon-Ktech Corporation, Tech Source Consulting, Texas Tech University, University of California at San Diego, University of Michigan at Ann Arbor, University of Missouri at Columbia, University of Nevada at Reno, University of New Mexico, University of Texas at Austin, Voss Scientific, Votaw Precision Technologies, and Weizmann Institute. This work was supported by the National Nuclear Security Administration, and the Laboratory Directed Research and Development Program at Sandia National Laboratories. Sandia is a multiprogram laboratory operated by Sandia Corporation, a Lockheed Martin Company, for the United States Department of Energy's National Nuclear Security Administration under Contract No. DE-AC04-94AL85000.

APPENDIX: OPTIMUM NEPTUNE-OUTPUT IMPEDANCE

In this Appendix we develop an estimate for the optimum value of $Z_{\rm out}$ for an accelerator such as Neptune. We use an idealized circuit model, one simpler than that given by Fig. 5. To develop the model, we make the following simplifying assumptions:

$$R_M \ll \sqrt{\frac{L_M}{C_M}}, \tag{A1}$$

$$R_{\rm radial} \ll Z_{\rm load}. \tag{A2}$$

When Eq. (A1) is applicable, the impedance $Z_{\rm in}$ that maximizes the peak forward-going power delivered by each Marx to the input of its associated coaxial-transmission-line impedance transformer is given by

$$Z_{\rm in} = 1.10\sqrt{\frac{L_M}{C_M}} = 1.10 n_b \sqrt{\frac{L_b}{C_b}}. \tag{A3}$$

In general, Neptune's 600 Marx generators are triggered at different times. Without loss of generality, we assume here that the 600 Marxes are triggered simultaneously. We also assume each coaxial impedance transformer is 100% efficient. In addition, we assume that for time scales of interest, the Marxes are transit time isolated from the centrally located system of conical transmission lines.

Under these assumptions, Fig. 5 can be approximated by the idealized circuit given by Fig. 10, where

$$L_{\rm center} \equiv L_{\rm con} + L_{\rm radial}. \tag{A4}$$

Dimensional analysis makes clear that the value of $Z_{\rm out}$ that maximizes the peak current delivered to the $Z_{\rm load}$ circuit element of Fig. 10 can be a function only of n_M, $Z_{\rm load}$, $L_{\rm center}$, and $(L_M C_M)^{1/2}$ [or equivalently, $(L_b C_b)^{1/2}$]. This observation, and Eq. (C18) of Ref. [43], lead to the following approximate expression for the optimum value of $Z_{\rm out}$:

$$Z_{\rm out} \approx n_M \left(Z_{\rm load} + \frac{0.55 L_{\rm center}}{\sqrt{L_b C_b}} \right). \tag{A5}$$

SCREAMER circuit simulations find that Eq. (A5) estimates to within 6% the optimum value of $Z_{\rm out}$ for the accelerator circuit given by Fig. 10. The value of $Z_{\rm out}$ given by Eq. (A5) achieves within 1% of the maximum possible value of the

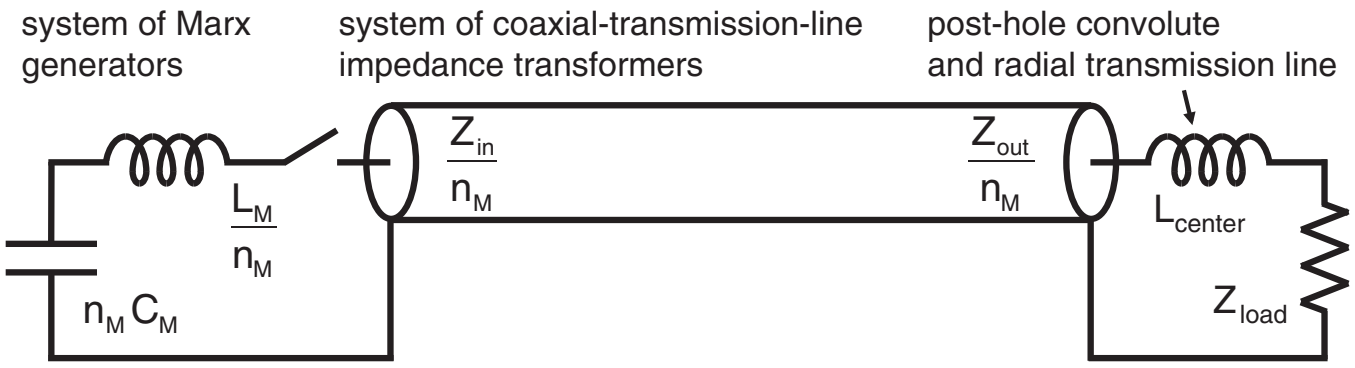

FIG. 10. Idealized version of the Neptune-circuit model illustrated by Fig. 5. The circuit presented here assumes all the Neptune Marx generators are triggered simultaneously.

peak load current. We observe that when $L_{center} = 0$, Eq. (A5) gives the result expected from elementary transmission-line theory; when $Z_{load} = 0$, Eq. (A5) is consistent with Eq. (C18) of [43].

[1] D. B. Reisman, A. Toor, R. C. Cauble, C. A. Hall, J. R. Asay, M. D. Knudson, and M. D. Furnish, Magnetically driven isentropic compression experiments on the Z accelerator, J. Appl. Phys. **89**, 1625 (2001).

[2] C. A. Hall, Isentropic compression experiments on the Sandia Z accelerator, Phys. Plasmas **7**, 2069 (2000).

[3] C. A. Hall, J. R. Asay, M. D. Knudson, W. A. Stygar, R. B. Spielman, T. D. Pointon, D. B. Reisman, A. Toor, and R. C. Cauble, Experimental configuration for isentropic compression of solids using pulsed magnetic loading, Rev. Sci. Instrum. **72**, 3587 (2001).

[4] R. B. Spielman, W. A. Stygar, J. F. Seamen, F. Long, H. Ives, R. Garcia, T. Wagoner, K. W. Struve, M. Mostrom, I. Smith, P. Spence, and P. Corcoran, Pulsed power performance of PBFA *Z*, in *Proceedings of the 11th IEEE International Pulsed Power Conference*, edited by G. Cooperstein and I. Vitkovitsky (IEEE, Piscataway, NJ, 1997), p. 709.

[5] K. W. Struve, T. H. Martin, R. B. Spielman, W. A. Stygar, P. A. Corcoran, and J. W. Douglas, Circuit-code modeling of the PBFA Z for z-pinch experiments, in *Proceedings of the 11th IEEE International Pulsed Power Conference*, edited by G. Cooperstein and I. Vitkovitsky (Ref. [4]), p. 162.

[6] I. D. Smith, P. A. Corcoran, W. A. Stygar, T. H. Martin, R. B. Spielman, and R. W. Shoup, Design criteria for the Z vacuum insulator stack, in *Proceedings of the 11th IEEE International Pulsed Power Conference*, edited by G. Cooperstein and I. Vitkovitsky (Ref. [4]), p. 168.

[7] M. A. Mostrom, T. P. Hughes, R. E. Clark, W. A. Stygar, and R. B. Spielman, IVORY PIC simulations of the Z insulator stack, in *Proceedings of the 11th IEEE International Pulsed Power Conference*, edited by G. Cooperstein and I. Vitkovitsky (Ref. [4]), p. 460.

[8] P. A. Corcoran, J. W. Douglas, I. D. Smith, P. W. Spence, W. A. Stygar, K. W. Struve, T. H. Martin, R. B. Spielman, and H. C. Ives, PBFA-*Z* vacuum section design using TLCODE simulations, in *Proceedings of the 11th IEEE International Pulsed Power Conference*, edited by G. Cooperstein and I. Vitkovitsky (Ref. [4]), p. 466.

[9] W. A. Stygar *et al.*, Design and performance of the Z magnetically-insulated transmission lines, in *Proceedings of the 11th IEEE International Pulsed Power Conference*, edited by G. Cooperstein and I. Vitkovitsky (Ref. [4]), p. 591.

[10] H. C. Ives, D. M. Van De Valde, F. W. Long, J. W. Smith, R. B. Spielman, W. A. Stygar, R. W. Wavrick, and R. W. Shoup, Engineering design of the Z magnetically-insulated transmission lines and insulator stack, in *Proceedings of the 11th IEEE International Pulsed Power Conference*, edited by G. Cooperstein and I. Vitkovitsky (Ref. [4]), p. 1602.

[11] R. W. Shoup, F. Long, T. H. Martin, R. B. Spielman, W. A. Stygar, M. A. Mostrom, K. W. Struve, H. Ives, P. Corcoran, and I. Smith, Design validation of the PBFA-Z vacuum insulator stack, in *Proceedings of the 11th IEEE International Pulsed Power Conference*, edited by G. Cooperstein and I. Vitkovitsky (Ref. [4]), p. 1608.

[12] R. J. Garcia, H. C. Ives, K. W. Struve, R. B. Spielman, T. H. Martin, M. L. Horry, R. Wavrik, and T. F. Jaramillo, Water-line design and performance of Z, in *Proceedings of the 11th IEEE International Pulsed Power Conference*, edited by G. Cooperstein and I. Vitkovitsky (Ref. [4]), p. 1614.

[13] R. B. Spielman *et al.*, Tungsten wire-array z-pinch experiments at 200 TW and 2 MJ, Phys. Plasmas **5**, 2105 (1998).

[14] T. C. Wagoner *et al.*, Differential-output B-dot and D-dot monitors for current and voltage measurements on a 20-MA, 3-MV pulsed-power accelerator, Phys. Rev. ST Accel. Beams **11**, 100401 (2008).

[15] W. A. Stygar *et al.*, 55-TW magnetically insulated transmission-line system: Design, simulations, and performance, Phys. Rev. ST Accel. Beams **12**, 120401 (2009).

[16] C. A. Jennings, M. E. Cuneo, E. M. Waisman, D. B. Sinars, D. J. Ampleford, G. R. Bennett, W. A. Stygar, and J. P. Chittenden, Simulations of the implosion and stagnation of compact wire arrays, Phys. Plasmas **17**, 092703 (2010).

[17] D. H. McDaniel, M. G. Mazarakis, D. E. Bliss, J. M. Elizondo, H. C. Harjes, H. C. Ives III, D. L. Kitterman,

J. E. Maenchen, T. D. Pointon, S. E. Rosenthal, D. L. Smith, K. W. Struve, W. A. Stygar, E. A. Weinbrecht, D. L. Johnson, and J. P. Corley, The ZR refurbishment project, in *Proceedings of the 5th International Conference on Dense Z Pinches*, edited by J. Davis, C. Deeney, and N. Pereira, AIP Conf. Proc. No. 651 (American Institute of Physics, Melville, NY, 2002), p. 23.

[18] T. D. Pointon and M. E. Savage, 2-D PIC simulations of electron flow in the magnetically insulated transmission lines of Z and ZR, in *Proceedings of the 15th IEEE International Pulsed Power Conference*, edited by J. Maenchen and E. Schamiloglu (IEEE, Piscataway, NJ, 2005), p. 151.

[19] T. D. Pointon, W. L. Langston, and M. E. Savage, Computer simulations of the magnetically insulated transmission lines and post-hole convolute of ZR, in *Proceedings of the 16th IEEE International Pulsed Power Conference*, edited by E. Schamiloglu and F. Peterkin (IEEE, Piscataway, NJ, 2007), p. 165.

[20] M. E. Savage *et al.*, An overview of pulse compression and power flow in the upgraded Z pulsed power driver, in *Proceedings of the 16th IEEE International Pulsed Power Conference*, edited by E. Schamiloglu and F. Peterkin (Ref. [19]), p. 979.

[21] K. R. LeChien, M. E. Savage, V. Anaya, D. E. Bliss, W. T. Clark, J. P. Corley, G. Feltz, J. E. Garrity, D. W. Guthrie, K. C. Hodge, J. E. Maenchen, R. Maier, K. R. Prestwich, K. W. Struve, W. A. Stygar, T. Thompson, J. Van Den Avyle, P. E. Wakeland, Z. R. Wallace, and J. R. Woodworth, Development of a 5.4 MV laser triggered gas switch for multimodule, multimegampere pulsed power drivers, Phys. Rev. ST Accel. Beams **11**, 060402 (2008).

[22] M. E. Savage and B. S. Stoltzfus, High reliability low jitter 80 kV pulse generator, Phys. Rev. ST Accel. Beams **12**, 080401 (2009).

[23] P. A. Corcoran, B. A. Whitney, V. L. Bailey, I. D. Smith, W. A. Stygar, M. E. Savage, G. A. Rochau, J. E. Bailey, B. M. Jones, T. J. Nash, M. E. Sceiford, L. G. Schlitt, and J. W. Douglas, Circuit modeling techniques applied to ZR, in *Proceedings of the 17th IEEE International Pulsed Power Conference* (IEEE, Piscataway, NJ, 2009), p. 150.

[24] B. Stoltzfus, K. LeChien, M. Savage, and W. Stygar, High voltage insulator improvements made in the oil and water sections of the Z machine at Sandia National Laboratories in 2008, in *Proceedings of the 17th IEEE International Pulsed Power Conference* (Ref. [23]), p. 425.

[25] D. V. Rose, D. R. Welch, R. E. Clark, E. A. Madrid, C. L. Miller, C. L. Mostrom, W. A. Stygar, M. E. Cuneo, C. A. Jennings, B. Jones, D. J. Ampleford, and K. W. Struve, ZR-convolute analysis and modeling: Plasma evolution and dynamics leading to current losses, in *Proceedings of the 17th IEEE International Pulsed Power Conference* (Ref. [23]), p. 1153.

[26] J. Lips, J. Garde, A. Owen, R. McKee, and W. Stygar, Modeling fluid/structural interaction in a pulsed power accelerator, in *Proceedings of the 17th IEEE International Pulsed Power Conference* (Ref. [23]), p. 1266.

[27] D. V. Rose, D. R. Welch, E. A. Madrid, C. L. Miller, R. E. Clark, W. A. Stygar, M. E. Savage, G. A. Rochau, J. E. Bailey, T. J. Nash, M. E. Sceiford, K. W. Struve, P. A. Corcoran, and B. A. Whitney, Three-dimensional electromagnetic model of the pulsed-power Z-pinch accelerator, Phys. Rev. ST Accel. Beams **13**, 010402 (2010).

[28] K. R. LeChien *et al.*, 6.1-MV, 0.79-MA laser-triggered gas switch for multimodule, multiterawatt pulsed-power accelerators, Phys. Rev. ST Accel. Beams **13**, 030401 (2010).

[29] M. E. Savage, K. R. LeChien, M. R. Lopez, B. S. Stoltzfus, W. A. Stygar, D. S. Artery, J. A. Lott, and P. A. Corcoran, Status of the Z pulsed power driver, in *Proceedings of the 18th IEEE International Pulsed Power Conference*, edited by R. D. Curry and B. V. Oliver (IEEE, Piscataway, NJ, 2011), p. 983.

[30] T. Ao, J. R. Asay, S. Chantrenne, M. R. Baer, and C. A. Hall, A compact strip-line pulsed power generator for isentropic compression experiments, Rev. Sci. Instrum. **79**, 013903 (2008).

[31] S. F. Glover, L. X. Schneider, K. W. Reed, G. E. Pena, J.-P. Davis, C. A. Hall, R. J. Hickman, K. C. Hodge, J. M. Lehr, D. J. Lucero, D. H. McDaniel, J. G. Puissant, J. M. Rudys, M. E. Sceiford, S. J. Tullar, D. M. Van De Valde, and F. E. White, Genesis: A 5-MA programmable pulsed-power driver for isentropic compression experiments, IEEE Trans. Plasma Sci. **38**, 2620 (2010).

[32] A. Lefrançois, P.-Y. Chanal, G. Le Blanc, J. Petit, G. Avrillaud, and M. Delchambre, High-velocity flyer-plate developments on two high-pulsed-power generators based on a strip-line design (GEPI and CEPAGE), IEEE Trans. Plasma Sci. **39**, 288 (2011).

[33] D. G. Tasker, C. H. Mielke, G. Rodriguez, and D. W. Rickel, Isentropic compression studies at the Los Alamos National High Magnetic Field Laboratory, in *Proceedings of the 18th IEEE International Pulsed Power Conference*, edited by R. D. Curry and B. V. Oliver (Ref. [29]), p. 1516.

[34] S. F. Glover *et al.*, Impact of time-varying loads on the programmable pulsed power driver called Genesis, IEEE Trans. Plasma Sci. **40**, 2588 (2012).

[35] S. F. Glover, F. E. White, P. J. Foster, D. J. Lucero, L. X. Schneider, K. W. Reed, G. E. Pena, J.-P. Davis, C. A. Hall, R. J. Hickman, K. C. Hodge, R. W. Lemke, J. M. Lehr, D. H. McDaniel, J. G. Puissant, J. M. Rudys, M. E. Sceiford, S. J. Tullar, and D. M. Van De Valde, Status of Genesis: A 5-MA programmable pulsed power driver, IEEE Trans. Plasma Sci. **40**, 2629 (2012).

[36] G. Wang, J. Zhao, H. Zhang, C. Sun, F. Tan, G. Wang, J. Mo, J. Cai, and G. Wu, Advances in quasi-isentropic compression experiments at Institute of Fluid Physics of CAEP, Eur. Phys. J. Spec. Top. **206**, 163 (2012).

[37] W. Stygar, R. Focia, W. Fowler, B. Hutsel, M. Mazarakis, J. Porter, S. Roznowski, M. Savage, and B. Stoltzfus, Conceptual design of a megabar-class accelerator for material-physics experiments, in *The Fourth Fundamental Science with Pulsed Power: Research Opportunities and User Meeting* (Sandia National Laboratories, Albuquerque, New Mexico, 2012).

[38] W. Stygar *et al.*, Conceptual designs of next-generation pulsed-power accelerators, in The 20th IEEE International Pulsed Power Conference, Sandia National Laboratories Report No. SAND2015-4846C, 2015.

[39] D. B. Reisman, B. S. Stoltzfus, W. A. Stygar, K. N. Austin, E. M. Waisman, R. J. Hickman, J.-P. Davis, T. A. Haill, M. D. Knudson, C. T. Seagle, J. L. Brown, D. A. Goerz, R. B. Spielman, J. A. Goldlust, and W. R. Cravey, Pulsed power accelerator for material physics experiments, Phys. Rev. ST Accel. Beams **18**, 090401 (2015).

[40] B. S. Stoltzfus, K. Austin, B. T. Hutsel, D. Reisman, M. E. Savage, and W. A. Stygar, Variable-pulse-shape pulsed-power accelerator, U.S. Patent Application US 2015/0366045 A1, 2015.

[41] E. M. Waisman, D. B. Reisman, B. S. Stoltzfus, W. A. Stygar, M. E. Cuneo, T. A. Haill, J.-P. Davis, J. L. Brown, C. T. Seagle, and R. B. Spielman, Optimization of current waveform tailoring for magnetically-driven isentropic compression experiments, Rev. Sci. Instrum. **87**, 063906 (2016).

[42] W. A. Stygar, M. E. Cuneo, D. I. Headley, H. C. Ives, R. J. Leeper, M. G. Mazarakis, C. L. Olson, J. L. Porter, T. C. Wagoner, and J. R. Woodworth, Architecture of petawatt-class z-pinch accelerators, Phys. Rev. ST Accel. Beams **10**, 030401 (2007).

[43] W. A. Stygar *et al.*, Conceptual designs of two petawatt-class pulsed-power accelerators for high-energy-density-physics experiments, Phys. Rev. ST Accel. Beams **18**, 110401 (2015).

[44] F. Gruner, W. Stygar, B. Stoltzfus, J. Woodworth, M. Abdalla, W. Gruner, M. Skipper, and S. Romero, A robust, low-inductance, low-jitter switch for petawatt-class pulsed power accelerators, in *The 19th IEEE International Pulsed Power Conference* (IEEE, Piscataway, NJ, 2013).

[45] I. A. D. Lewis and F. H. Wells, *Millimicrosecond Pulse Techniques* (Pergamon Press, New York, 1959).

[46] D. R. Welch, T. C. Genoni, D. V. Rose, N. L. Bruner, and W. A. Stygar, Optimized transmission-line impedance transformers for petawatt-class pulsed-power accelerators, Phys. Rev. ST Accel. Beams **11**, 030401 (2008).

[47] M. L. Kiefer and M. M. Widner, SCREAMER—a single-line pulsed-power design tool, in *Proceedings of the 5th IEEE International Pulsed Power Conference*, edited by M. F. Rose and P. J. Turchi (IEEE, Piscataway, NJ, 1985), p. 685.

[48] R. B. Spielman, M. L. Kiefer, K. L. Shaw, K. W. Struve, and M. M. Widner, SCREAMER, A pulsed power design tool, User's guide for version 3.3.2 (2014).

[49] R. B. Spielman and Y. Gryazin, SCREAMER V4.0—a powerful circuit analysis code, in *Proceedings of the 20th IEEE International Pulsed Power Conference* (IEEE, Piscataway, NJ, 2015), p. 1.

[50] M. E. Savage, Balanced two-capacitor brick for linear transformer drivers (unpublished).

[51] W. A. Stygar, S. E. Rosenthal, H. C. Ives, T. C. Wagoner, G. O. Allshouse, K. E. Androlewicz, G. L. Donovan, D. L. Fehl, M. H. Frese, T. L. Gilliland, M. F. Johnson, J. A. Mills, D. B. Reisman, P. G. Reynolds, C. S. Speas, R. B. Spielman, K. W. Struve, A. Toor, and E. M. Waisman, Energy loss to conductors operated at lineal current densities $\leq$10 MA/cm: Semianalytic model, magnetohydrodynamic simulations, and experiment, Phys. Rev. ST Accel. Beams **11**, 120401 (2008).

[52] W. A. Stygar, T. C. Wagoner, H. C. Ives, Z. R. Wallace, V. Anaya, J. P. Corley, M. E. Cuneo, H. C. Harjes, J. A. Lott, G. R. Mowrer, E. A. Puetz, T. A. Thompson, S. E. Tripp, J. P. VanDevender, and J. R. Woodworth, Water-dielectric-breakdown relation for the design of large-area multimegavolt pulsed-power systems, Phys. Rev. ST Accel. Beams **9**, 070401 (2006).

[53] W. A. Stygar, M. E. Savage, T. C. Wagoner, L. F. Bennett, J. P. Corley, G. L. Donovan, D. L. Fehl, H. C. Ives, K. R. LeChien, G. T. Leifeste, F. W. Long, R. G. McKee, J. A. Mills, J. K. Moore, J. J. Ramirez, B. S. Stoltzfus, K. W. Struve, and J. R. Woodworth, Dielectric-breakdown tests of water at 6 MV, Phys. Rev. ST Accel. Beams **12**, 010402 (2009).